Signatures of charge inhomogeneities in the infrared spectra of topological insulators Bi_2Se_3, Bi_2Te_3 and Sb_2Te_3

2013 J. Phys.: Condens. Matter 25 075501

(http://iopscience.iop.org/0953-8984/25/7/075501)

J. Phys.: Condens. Matter **25** (2013) 075501 (5pp) doi:10.1088/0953-8984/25/7/075501

Signatures of charge inhomogeneities in the infrared spectra of topological insulators Bi_2Se_3, Bi_2Te_3 and Sb_2Te_3

S V Dordevic[1], M S Wolf[1], N Stojilovic[2], Hechang Lei[3] and C Petrovic[3]

[1] Department of Physics, University of Akron, Akron, OH 44325, USA
[2] Department of Physics and Astronomy, University of Wisconsin Oshkosh, Oshkosh, WI 54901, USA
[3] Condensed Matter Physics and Materials Science Department, Brookhaven National Laboratory, Upton, NY 11973, USA

E-mail: dsasa@uakron.edu (S V Dordevic)

Received 5 September 2012, in final form 29 November 2012
Published 17 January 2013
Online at stacks.iop.org/JPhysCM/25/075501

Abstract
We present the results of an infrared spectroscopy study of topological insulators Bi_2Se_3, Bi_2Te_3 and Sb_2Te_3. Reflectance spectra of all three materials look similar, with a well defined plasma edge. However, there are some important differences. Most notably, as temperature decreases the plasma edge shifts to lower frequencies in Bi_2Se_3, whereas in Bi_2Te_3 and Sb_2Te_3 it shifts to higher frequencies. In the loss function spectra we identify asymmetric broadening of the plasmon, and assign it to the presence of charge inhomogeneities. It remains to be seen if charge inhomogeneities are characteristic of all topological insulators, and whether they are of intrinsic or extrinsic nature.

(Some figures may appear in colour only in the online journal)

1. Introduction

Topological insulators (TI) are novel electronic materials that behave like ordinary insulators in the bulk, but have conducting states on the surface [1, 2]. Their unusual properties are believed to originate from strong spin–orbit coupling. Conducting states on the surface are protected by time-reversal symmetry and are characterized by linear carrier dispersion, represented with Dirac cones. It has been shown that unique properties of TI stem from the fact that they have an odd number (usually one) of cones per unit cell [1, 2].

Based on recent terahertz Kerr measurements on Bi_2Se_3 [3] it was suggested that bulk charge distribution might not be uniform, and that signatures of those inhomogeneities might be observable in the infrared spectra. To address this issue we conducted a comprehensive infrared study of several 'second generation' TI, with the goal of probing their electrodynamic properties under identical experimental conditions. Our results reveal that charge inhomogeneities are indeed present in TI and are particularly pronounced in Bi_2Se_3. The results also confirm that IR spectroscopy can be used for detecting such inhomogeneities, in a contactless and non-destructive way.

2. Results and discussion

Single crystals of Bi_2Se_3, Bi_2Te_3 and Sb_2Te_3 for this study were grown by the flux method [4, 5]. Samples with layered structure and irregular shapes were produced. Most of them had at least one naturally flat surface, with typical surface area of approximately 3 mm × 3 mm, and thickness of several millimeters. All spectroscopic measurements were performed on these flat surfaces. X-ray diffraction (XRD) spectra were taken with Cu Kα radiation ($\lambda = 0.154\,18$ nm) using a Rigaku Miniflex x-ray machine. Unit cell refinement obtained by fitting the XRD spectra using the Rietica software showed that samples were single phase and with lattice parameters consistent with previous results [6].

DC resistivity is measured using a four-point probe setup and the results are shown in figure 1(a). All three samples display characteristic metallic behavior, which correlates with behavior of carrier scattering rate $1/\tau(\omega)$ and plasma

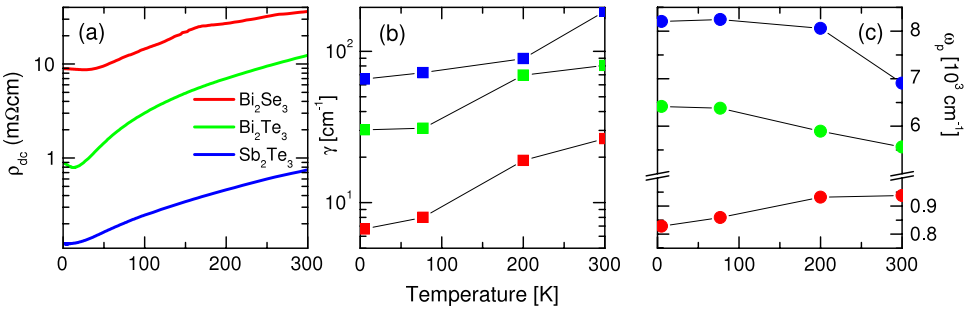

Figure 1. (a) Temperature dependence of DC resistivity of Bi_2Se_3, Bi_2Te_3 and Sb_2Te_3 on a semi-log plot. All three materials display metallic behavior, i.e. their resistivity decreases with temperature. (b) Scattering rate γ from the DL fits equation (2); in all three compounds scattering rate monotonically decreases with temperature. (c) Plasma frequency ω_p from the DL fits. Note that the in Bi_2Se_3 the plasma frequency increases with increasing temperature, whereas in Bi_2Te_3 and Sb_2Te_3 it decreases.

frequency ω_p extracted from IR spectra (see below) and shown in figures 1(b) and (c). The resistivity of Bi_2Se_3 displays characteristic shape observed previously [7]. Compared to [7], both in terms of absolute values and temperature dependence, our sample is closest to sample *vi* for which the carrier density was estimated based on Shubnikov–de Haas (SdH) measurements to be approximately 10^{16} cm^{-3}. Similar to that sample, the resistivity of our sample also displays a shallow minimum around 30 K. However, our sample does not display the downturn of resistivity at high temperatures, which indicates that the carrier density is higher than 10^{16} cm^{-3}, and this will indeed be revealed by our IR measurements.

The shape of resistivity of Bi_2Te_3 is qualitatively similar to that of Bi_2Se_3, but overall it is lower by approximately an order of magnitude. Assuming similar scattering rates, this indicates that the carrier density is higher in Bi_2Te_3, consistent with IR measurements (figure 1(c)). The resistivity of Bi_2Te_3 also displays a shallow, but more pronounced, minimum around 15 K. The resistivity of Sb_2Te_3 is even lower, indicating even higher carrier density. This sample does not display a shallow minimum at low temperatures, similar to Bi_2Se_3 samples with carrier densities higher than 10^{18} cm^{-3} [7].

Infrared spectra of Bi_2Se_3, Bi_2Te_3 and Sb_2Te_3 are reported over a broad range of frequencies and temperatures from 300 K down to 10 K. All measurements have been performed on natural, freshly cleaved surfaces to minimize exposure to air. Reflectance spectra were collected with the electric field vector oriented along the cleaved surfaces to probe the in-plane charge dynamics. An overcoating technique, with gold or aluminum coating of the sample as reference, was used to obtain the absolute values of reflectance [8]. The results are shown in figure 2 for all three materials, and they all display a well defined plasma edge, consistent with previous reports [7, 9–11]. This characteristic shape of reflectance is a consequence of zero crossing in the real part of the dielectric function [12] that occurs at the so called renormalized plasma frequency ω_p^*, which, on the other hand, is related to the carrier density n as:

$$\omega_p^{*2} = \frac{4\pi n e^2}{m^* \epsilon_\infty}. \qquad (1)$$

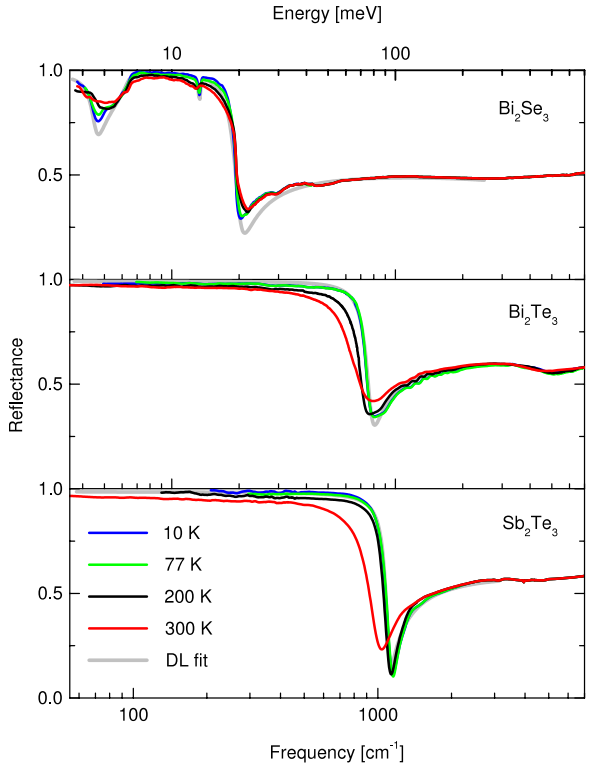

Figure 2. Reflectance spectra of Bi_2Se_3, Bi_2Te_3, and Sb_2Te_3. All three compounds display well defined plasma edge, which sharpens as temperature decreases. As temperature decreases the plasma minimum is shifting to lower frequencies in Bi_2Se_3, whereas in Bi_2Te_3 and Sb_2Te_3 it is shifting to higher frequencies. In Bi_2Se_3 we observe two strong phonon modes, which are not observed in Bi_2Te_3 and Sb_2Te_3. The Drude–Lorentz fits (equation (2)) are shown with gray lines.

In this expression m^* is the carrier effective mass and ϵ_∞ is the high-frequency dielectric function. The position of the edge progressively shifts from approximately 190 cm^{-1} in Bi_2Se_3, to 735 cm^{-1} in Bi_2Te_3, to 1045 cm^{-1} in Sb_2Te_3. We note that the plasma edge in Bi_2Se_3 is somewhat higher than for sample *iv* in [7] (approximately 160 cm^{-1}), but lower than in [9] (approximately 400 cm^{-1}) and [10] (approximately 500 cm^{-1}).

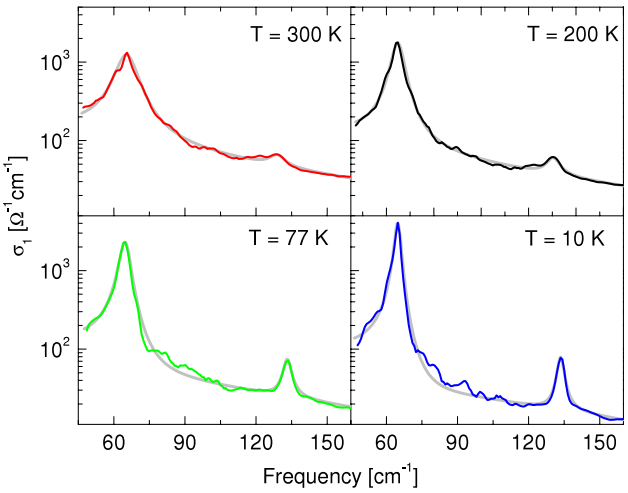

Figure 3. Real part of optical conductivity $\sigma_1(\omega)$ of Bi_2Se_3 along with the best fits (gray lines). Note that the vertical axis is logarithmic. The 133 cm^{-1} phonon mode is fit with a Lorentzian. On the other hand, the 65 cm^{-1} mode is asymmetric and at 10 and 77 K must be fit as a Fano resonance. At 300 and 200 K the asymmetry is small and a Lorentzian would produce equally good fits.

As temperature decreases the plasma edge sharpens in all three materials. In addition, the plasma minimum shifts, but interestingly these shifts are not in the same direction in all three compounds. In Bi_2Se_3 the plasma minimum shifts to lower frequencies (softens), whereas in Bi_2Te_3 and Sb_2Te_3 it shifts to higher frequencies (hardens) as temperature decreases. The softening of the plasmon in Bi_2Se_3 was observed in both [7, 9] but was not discussed.

Applying Kramers–Kronig transformation on the raw reflectance spectra we calculate other optical functions, such as the optical conductivity $\tilde{\sigma}(\omega) = \sigma_1(\omega) + i\sigma_2(\omega)$, and the dielectric function $\tilde{\epsilon}(\omega) = \epsilon_1(\omega) + i\epsilon_2(\omega)$. The real part of optical conductivity $\sigma_1(\omega)$ is particularly useful because it reveals the presence of transverse modes in solids. The optical conductivity of all three compounds display a well defined Drude-like mode, followed by contributions from interband transitions at higher energies. IR active phonon modes are also identified in the spectra of Bi_2Se_3 at 65 and 133 cm^{-1} (figure 3), in agreement with previous measurements [9, 7, 10, 13]. Interestingly no phonon modes are observed in Bi_2Te_3 and Sb_2Te_3 down to the lowest measured temperature. One can argue that the phonons are better screened because the latter two compounds are more conducting, i.e. their carrier density is higher.

To gain better understand of the electronic properties we fit the spectra with the Drude–Lorentz model [12, 14, 15]:

$$\epsilon(\omega) = \epsilon_\infty - \frac{\omega_p^2}{\omega^2 + i\gamma\omega} + \sum_{i=1}^{N} \frac{\omega_{p,i}^2}{\omega_{0,i}^2 - \omega^2 - i\gamma_i\omega}, \qquad (2)$$

where the second term is the Drude contribution due to free charge carriers, whereas the last term is due to finite frequency excitations, such as phonons and interband transitions. Since no phonons could be identified in the spectra of Bi_2Te_3 and Sb_2Te_3 only the first two terms in equation (2) are used. The fitting was done over the 35–2500 cm^{-1} range, using the program RefFIT [16]. Examples of the best fits at 10 K are shown with gray lines in figure 2.

From the best fits we extract the plasma frequency of charge carriers ω_p, as well as the carrier scattering rate γ. Obtained values for all three compounds are shown in figures 1(b) and (c)[4]. As can be seen, the scattering rate monotonically decreases with temperature in all three compounds and this explains the metallic behavior observed in resistivity (figure 1(a)). The plasma frequency on the other hand decreases by approximately 10% in Bi_2Se_3 between room temperature and 10 K, but increases by 15% in Bi_2Te_3 and by almost 20% in Sb_2Te_3, consistent with the observed temperature dependence of the plasmon (figure 2). We speculate that observed opposite trends in the temperature dependence of ω_p might be related to different type of charge carriers present. Namely, it has been known that charge carriers in Bi_2Se_3 are electron-like [7], whereas in Bi_2Te_3 and Sb_2Te_3 they are predominantly hole-like [17, 18].

From the plasma frequency ω_p one can in principle calculate carrier density, if their effective mass is know (equation (1)). In [7] the effective mass of charge carriers was determined for Bi_2Se_3 based on SdH measurements, and the value of $m^* = 0.15\ m_e$ was obtained. Assuming the same value for all three compounds[5], and using a three-dimensional free electron gas model [19], we extract the carrier density of 1.1×10^{18} cm^{-3} for Bi_2Se_3, 6.9×10^{19} cm^{-3} for Bi_2Te_3 and 1.1×10^{20} cm^{-3} for Sb_2Te_3.

Figure 3 displays the far-IR optical conductivity $\sigma_1(\omega)$ of Bi_2Se_3 on semi-log scale. The spectra reveal two phonon modes at all temperatures. However the 65 cm^{-1} mode displays considerable asymmetry and no good fits could be obtained with a Lorentzian. Following LaForge *et al* [9] we fit this mode with the Fano model, and the results of the fits are shown with gray lines in figure 3. At higher temperatures (300 and 200 K) the best fits yield for the Fano parameter q large values (typically $q \approx -30$) which indicates that there is very little asymmetry. On the other hand at low temperatures (77 and 10 K) the value of the Fano parameter is approximately -15, in agreement with LaForge *et al* [9]. Phonon asymmetry is commonly observed in systems with correlated electrons and is usually assigned to coupling of these modes to collective electron excitations. In the case of Bi_2Se_3 it was argued that the 65 cm^{-1} mode is coupled to the plasmon at higher energies (figure 4 bellow), yielding negative values of Fano parameter q. We also note that the positions (ω_0 in equation (2)) of both two phonon modes display small temperature dependences, although in different directions: 65 cm^{-1} mode softens slightly as temperature decreases, whereas the 133 cm^{-1} mode hardens.

Plasmon is a longitudinal mode and the real part of the optical conductivity $\sigma_1(\omega)$ does not couple to it. Instead,

[4] The values of other fitting parameters (at 10 K) from equation (2), not shown in figure 1, are as follows: for Bi_2Se_3 $\epsilon_\infty = 9$, $\omega_{0,ph} = 64$ cm^{-1}, $\omega_{p,ph} = 832$ cm^{-1} and $\gamma_{ph} = 3$ cm^{-1}, for Bi_2Te_3 $\epsilon_\infty = 64$, and for Sb_2Te_3 $\epsilon_\infty = 42$.

[5] The assumption that the effective mass is the same in all three compounds is questionable, but since the actual measurements on Bi_2Te_3 and Sb_2Te_3 are not available, we are forced to use it.

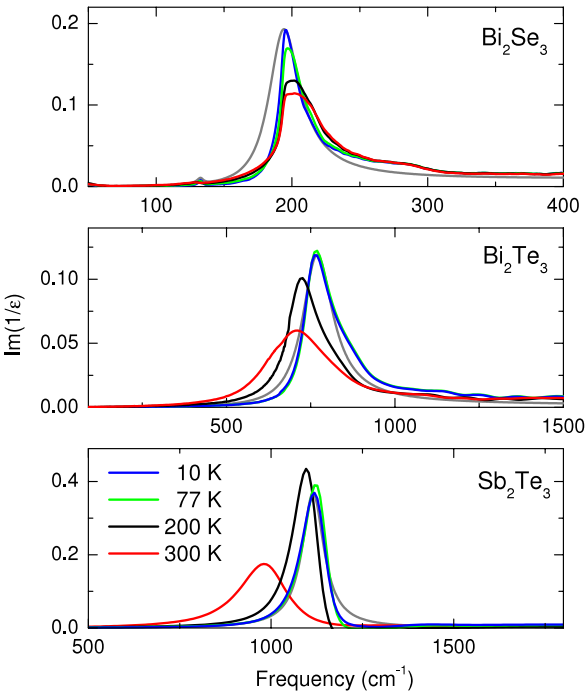

Figure 4. Loss function of Bi_2Se_3, Bi_2Te_3 and Sb_2Te_3 at several temperatures. In Bi_2Se_3 the plasmon shifts to lower frequencies as temperature decreases, whereas in Bi_2Te_3 and Sb_2Te_3 it shifts to higher frequencies. We also note considerable asymmetry in the shape of the peak, which might indicate the presence of charge inhomogeneities. Gray lines are fits to the Drude–Lorentz model (equation (2)).

in figure 4 we display the loss function $\mathrm{Im}[1/\epsilon(\omega)]$ for all three samples. The loss function reveals the presence of longitudinal modes, such as plasmons, in the optical spectra. As can be seen from figure 4 the plasmon is temperature dependent in all three compounds, but as anticipated from the raw reflectance data in Bi_2Se_3 it shifts to lower, whereas in Bi_2Te_3 and Sb_2Te_3 it shifts to higher frequencies as temperature decreases. We also note significant asymmetry (deviation from the expected Lorentzian-like shape) of the plasmon observed in the loss function $\mathrm{Im}[1/\epsilon(\omega)]$ (figure 4). For all three compounds we could not obtain a good fit around the plasmon, as it was not possible to achieve simultaneously good fit at the frequencies below and above the plasmon. Examples of these fits (equation (2)) are shown with gray lines in figure 4 for all three compounds at 10 K. The fit is especially poor in Bi_2Se_3 (see also figure 2). Similar problem was noted in [10] but was not discussed.

It has previously been argued that the asymmetry of collective modes revealed by the loss function is due to electronic inhomogeneities [20, 21]. The shape of the loss function spectra presented in figure 4 indicates that charge inhomogeneities are also present in Bi_2Se_3, Bi_2Te_3 and Sb_2Te_3, as previously speculated based on terahertz Kerr measurements [3]. To obtain quantitative information about the asymmetry, we follow Van der Marel and Tsvetkov [20] who suggested the following expression for the complex dielectric function $\epsilon(\omega)$ in the presence of inhomogeneities:

$$\frac{1}{\epsilon(\omega)} = \int_0^\infty \frac{1}{\epsilon_i(\omega, \omega_\mathrm{p})} \rho(\omega_\mathrm{p})\, \mathrm{d}\omega_\mathrm{p} \qquad (3)$$

where $\rho(\omega_\mathrm{p})$ is the distribution function of plasma frequencies and $\epsilon_i(\omega, \omega_\mathrm{p})$ is the complex dielectric function for each individual component, given by equation (2). Instead of assuming a particular form for the distribution function (Gaussian, for example [20, 21]), we numerically solve equation (3) and calculate $\rho(\omega_\mathrm{p})$ from the experimental loss function. This is an inverse problem, and its solution requires special numerical techniques [22]. We employ the histogram method [23], in which the solution is represented with N blocks whose heights are the unknown fitting parameters, to be determined from the numerical procedure. Block coordinates (and therefore block widths) are not fitting parameters, and have been specified beforehand to match the approximate shape of the distribution function $\rho(\omega_\mathrm{p})$. The heights of the blocks were optimized using the Levenberg–Marquardt algorithm, with the goal of minimizing the error function [22]. We estimate the error bars of the solutions to be about $\pm 10\%$.

The results of our calculations are shown in figure 5 for all three compounds[6]. The distribution functions $\rho(\omega_\mathrm{p})$ are normalized to their maximum values, and the frequency values are normalized to the central frequency of the distribution $\omega_\mathrm{p}/\omega_0$. The values of carrier density n, calculated from equation (1), are also shown on top axis. As anticipated from the loss function, the distribution is narrow and almost symmetric in Sb_2Te_3. In Bi_2Te_3 the distribution is somewhat broadened and slightly asymmetric. However, in Bi_2Se_3 significant broadening and asymmetry of $\rho(\omega_\mathrm{p})$ are observed: calculated distribution is as wide as 10%. We speculate that the broadening and asymmetry of the plasmon are much smaller in Bi_2Te_3 and Sb_2Te_3 because of a different type of charge carriers (holes, as opposed to electrons).

The above calculations imply presence of charge inhomogeneities, especially in Bi_2Se_3, but based on these calculations one cannot distinguish if the inhomogeneities are intrinsic to topological insulators[7], or if they are due to sample imperfections, such as impurities, defects, disorder etc. Recent tunneling measurements [25, 26] indicate that surface charge distribution is fairly uniform. However, IR measurements primarily probe bulk carriers, whose properties can be quite different from those on the surface. Terahertz Kerr measurements on Bi_2Se_3 [3], which first suggested the existence of charge inhomogeneities, could not elucidate the true nature of these inhomogeneities either. Alternative approaches might be needed to address this important question.

3. Summary

In summary, we presented IR spectra of three 'second generation' topological insulators Bi_2Se_3, Bi_2Te_3 and Sb_2Te_3. The spectra reveal peculiar temperature dependence of

[6] The values of other parameters from equation (2),which where kept constant during the optimization procedure, are as follows: for Bi_2Se_3 $\epsilon_\infty = 9$ and $\gamma = 13$ cm^{-1}, for Bi_2Te_3 $\epsilon_\infty = 64$ and $\gamma = 30$ cm^{-1}, and for Sb_2Te_3 $\epsilon_\infty = 42$ and $\gamma = 72$ cm^{-1}.

[7] Signatures of charge inhomogeneities were also noticed in the infrared spectra of another topological insulator, $Bi_{0.91}Sb_{0.09}$ [24].

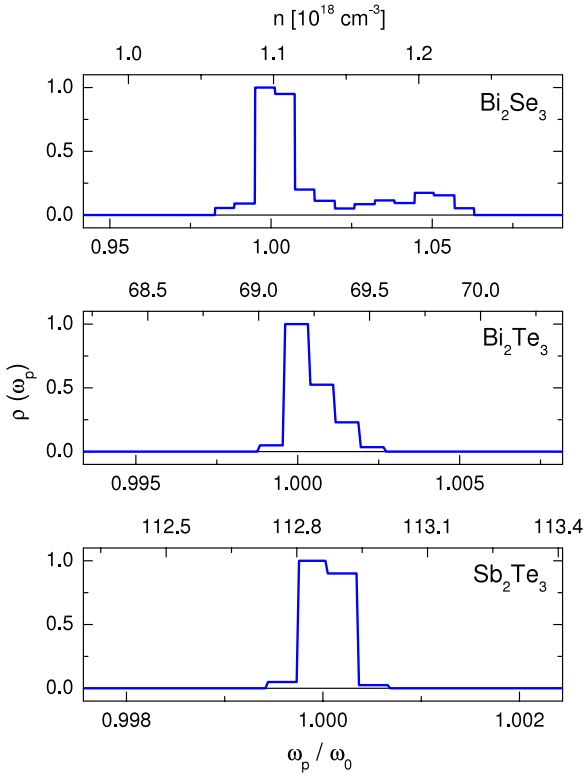

Figure 5. Histogram representation of the distribution function of plasma frequencies $\rho(\omega_p)$, shown as a function of normalized plasma frequency ω_p/ω_0 (bottom axes), as well as carrier density n (top axes). The distribution function of plasma frequencies $\rho(\omega_p)$ was calculated from the loss function data at 10 K (figure 4). For the purpose of comparison, the distribution functions are normalized to their maximum values.

the plasmon in the three compounds. The analysis of the loss function spectra reveals the presence of charge inhomogeneities, most notably in Bi_2Se_3. Further studies will be needed to check if they are characteristic of all topological insulators, and if they are of intrinsic or extrinsic nature.

Acknowledgments

The authors thank D N Basov, A D LaForge and A A Schafgans for useful discussions. SVD acknowledges the support from The University of Akron FRG. Special thanks to R Ramsier for the use of his equipment. Work at Brookhaven is supported by the US DOE under Contract No. DE-AC02-98CH10886 (HL and CP).

References

[1] Hasan M Z and Kane C L 2010 *Rev. Mod. Phys.* **82** 3045
[2] Qi X L and Zhang S C 2011 *Rev. Mod. Phys.* **83** 1057
[3] Jenkins G S, Sushkov A B, Schmadel D C, Butch N P, Syers P, Paglione J and Drew H D 2010 *Phys. Rev.* B **82** 125120
[4] Fisk Z and Remeika J P 1989 *Handbook on the Physics and Chemistry of Rare Earths* vol 12, ed K A Gschneider and J Eyring (Amsterdam: Elsevier)
[5] Canfield P C and Fisk Z 1992 *Phil. Mag.* B **65** 1117
[6] Hunter B 1998 Rietica—a visual Rietveld program *International Union of Crystallography Commission on Powder Diffraction Newsletter* No. 20 (Summer)
[7] Butch N P, Kirshenbaum K, Syers P, Sushkov A B, Jenkins G S, Drew H D and Paglione J 2010 *Phys. Rev.* B **81** 241301
[8] Homes C C, Reedyk M A, Crandles D A and Timusk T 1993 *Appl. Opt.* **32** 2976
[9] LaForge A D, Frenzel A, Pursley B C, Lin T, Liu X, Shi J and Basov D N 2010 *Phys. Rev.* B **81** 125120
[10] Sushkov A B, Jenkins G S, Schmadel D C, Butch N P, Paglione J and Drew H D 2010 *Phys. Rev.* B **82** 125110
[11] Di Pietro P, Vitucci F M, Nicoletti D, Baldassarre L, Calvani P, Cava R, Hor Y S, Schade U and Lupi S 2012 *Phys. Rev.* B **86** 045439
[12] Dressel M and Gruner G 2001 *Electrodynamics of Solids* (Cambridge: Cambridge University Press)
[13] Valdes Aguilar R *et al* 2012 *Phys. Rev. Lett.* **108** 087403
[14] Basov D N and Timusk T 2005 *Rev. Mod. Phys.* **77** 721
[15] Dordevic S V and Basov D N 2006 *Ann. Phys., Lpz.* **15** 545
[16] Kuzmenko A B 2005 *Rev. Sci. Instrum.* **76** 083108
[17] Hor Y S, Qu D, Ong N P and Cava R J 2010 *J. Phys.: Condens. Matter* **22** 375801
[18] Eichler W and Krug T 1980 *Phys. Status Solidi* b **101** K1
[19] Ashcroft N W and Mermin N D 1976 *Solid State Physics* (Stamford, CT: Brooks/Cole)
[20] Van der Marel D and Tsvetkov A 1996 *Czech. J. Phys.* **46** 3165
[21] Dordevic S V, Komiya S, Ando Y and Basov D N 2003 *Phys. Rev. Lett.* **91** 167401
[22] Press W H, Teukolsky S A, Vetterling W T and Flannery B P 2002 *Numerical Recipes* (Cambridge: Cambridge University Press) and references therein
[23] Van Heumen E, Muhlethaler E, Kuzmenko A B, Eisaki H, Meevasana W, Greven M and van der Marel D 2009 *Phys. Rev.* B **79** 184512
[24] Schafgans A A, LaForge A D, Taskin A, Ando Y and Basov D N 2011 *APS March Meeting (Dallas, TX, Mar. 2011)* vol 56 no. 1 (*Session J 35: Topological Insulators: Optics*) J 35.00003 http://meetings.aps.org/link/BAPS.2011.MAR.J35.3
[25] Zhang T *et al* 2009 *Phys. Rev. Lett.* **103** 266803
[26] West D, Sun Y Y, Zhang S B, Zhang T, Ma X, Cheng P, Zhang Y Y, Chen X, Jia J F and Xue Q K 2012 *Phys. Rev.* B **85** 081305